Journal of the European Ceramic Society 22 (2002) 109–119

www.elsevier.com/locate/jeurceramsoc

The effect of processing conditions, amount of additives and composition on the microstructures and mechanical properties of α-SiAlON ceramics

S. Kurama [a], M. Herrmann [b], H. Mandal [a,*]

[a] *Anadolu University, Department of Ceramic Engineering, Iki Eylul Campus, Eskisehir, 26470, Turkey*
[b] *Fraunhofer Institut Keramische Technologien und Sinterwerkstoffe, D-01277 Dresden, Germany*

Received 14 December 2000; received in revised form 10 February 2001; accepted 16 February 2001

Abstract

A series of samples with yttrium α-SiAlON compositions and different amounts of additive has been fabricated from α-Si_3N_4, AlN, Al_2O_3 and Y_2O_3 starting powders, using gas pressure sintering and three different sintering procedures. One series of samples was heated up to 1825°C and then held for 3 h, another group of samples was held at a lower temperature (1500 or 1600°C) for 1 h and then heated up to 1825°C and held for 3 h. The results of investigations using scanning electron microscopy showed the effect of composition and sintering procedure on the morphology of α-SiAlON grains. It was found that the amount of elongated grains increased with increasing amount of liquid phase. The mechanical tests showed that all of the samples exhibited HV10 values in the range of 1800–1976 kg/mm and K_{IC} values in the range of 3.9–6.3 $MPam^{1/2}$.

Keywords: Grain morphology; Mechanical properties; Microstructure-final; SiAlONs; Sintering

1. Introduction

Until recently, the development of single phase α-SiAlON ceramics has received little attention. This has primarily been due to the poor fracture toughness and processing difficulties associated with the fabrication of these materials. Conversely, β-SiAlON ceramics are easier to densify than α-SiAlON by pressureless sintering and possess a good combination of properties, among which is the relatively high toughness that arises from the elongated morphology of β-SiAlON grains.[1]

It is well established that the presence of elongated grains gives rise to mechanisms such as crack deflection, crack bridging and grain pullout, which improve fracture toughness and reliability.[2] It is well known that α-SiAlON with a composition of $M_xSi_{12-(m+n)}Al_{m+n}O_nN_{16-n}$, where $x=m/v$ and M^{+v} = Li, Mg, Ca, Y and some rare earth elements is generally considered to occur in an equiaxed grain morphology,[3] and thus, its toughness is much lower than that of β-SiAlON. On the other hand, α-SiAlON has the advantage of a significantly higher hardness than that of β-SiAlON.

There are very few reports on the formation of elongated α-SiAlON grains, but recent studies of different rare earth doped α-SiAlON compositions have revealed that elongated α-SiAlON grains can be formed under certain preparative condition.[4–8] The first example was given by Hwang et al., who observed anisotropic grain growth of the α-SiAlON phase when different sintering aids (CaO, SrO and Y_2O_3) were used simultaneously.[4] Later Wang et al.,[5] Nordberg et al.,[6] and Mandal[8] showed that CaO, rare earth and mix cation additions also formed elongated α-SiAlON. Analysis of the composition of the α-SiAlON materials with elongated grains, shows that they have relative large n and m values[9] (Fig. 1). Therefore, the formation of elongated α-SiAlON grains was mostly connected with the existence of enough liquid phase during the sintering process. An increase in the SiO_2 or Al_2O_3 content in comparison to that of the pure α-SiAlON composition does not give very reliable results, due to the small weight losses occurring during sintering, which changed the densification behaviour. That is why in the present work an additional amount of Y_2O_3 in comparison to

* Corresponding author. Tel.: +90-222-321-3550, ext. 6351; fax: +90-222-323-9501.
E-mail address: hmandal@mmf.mmanadolu.edu.tr (H. Mandal).

0955-2219/01/$ - see front matter
PII: S0955-2219(01)00237-0

the amount in the α-SiAlON composition was chosen to obtain a stable liquid phase and to accelerate the formation of elongated grains. The most attractive results were reported by Chen and Rosenflanz in *Nature* in 1997.[7] They used β-Si_3N_4 as a starting powder to synthesise α-SiAlON and prove that also the Si_3N_4 type effects grains form.

In the present work, the effect of the different processing conditions, amount of the additive (Y_2O_3) and composition on the morphology of the Y-α-SiAlON grains was examined. The factors that affect the formation of elongated-Y-α-SiAlON grains are discussed.

Table 1
Starting composition and corresponding *n*, *m* and *K* values

Samples	*m* value	*n* value	Composition (wt.%)				
			K[a]	Si_3N_4	AlN	Al_2O_3	Y_2O_3
ZY 1	0.44	0.76	1	88.66	8.63	0.008	2.89
ZY 1b			1.43	87.57	8.52	0.008	4.08
ZY 1f			2.36	85.10	8.31	–	6.58
ZY 2	0.59	0.98	1	84.79	10.44	0.93	3.84
ZY 2b			1.43	83.43	10.27	0.93	5.38
ZY 2c			1.61	82.84	10.21	0.93	6.03
ZY 2e			1.94	81.83	10.08	0.93	7.16
ZY 3	0.91	0.98	1	80.90	13.25	0.0043	5.84
ZY 3b			1.43	78.92	12.96	–	8.12
ZY 3d			1.69	77.73	12.77	–	9.5
ZY 4	1.12	1.17	1	76.88	15.44	0.55	7.12
ZY 4a			1.2	75.73	15.21	0.54	8.51
ZY 4b			1.43	74.65	14.99	0.54	9.81
ZY 5	0.86	1.26	1	79.23	13.42	1.84	5.51
ZY 6	1	1.26	1	77.59	14.6	1.43	6.34
ZY 7	1.16	1.26	1	75.72	15.98	0.97	7.33
ZY 8	1.0	1.5	1	75.62	15.12	2.87	6.39
ZY 9	1.4	1.5	1	71.07	18.47	1.71	8.75
ZY 10	1.8	1.5	1	66.67	21.68	0.60	11.05

[a] *K*: ratio of amount of Y_2O_3 to amount of Y_2O_3 incorporated into α-SiAlON.

2. Experimental

Different α-SiAlON compositions were prepared using the following starting powders α-Si_3N_4 (UBE-10, containing 1.6% oxygen), AlN (Tokuyama, containing 1% oxygen), Al_2O_3 (99.99%, AKP50) and Y_2O_3 (99.99% HC Starck). The oxygen contents of the nitride powders were taken into account in calculating the compositions (Table 1). To obtain different compositions in the α-SiAlON/β-SiAlON plane, additional amounts of Y_2O_3 were added. This additional Y_2O_3, which can not be incorporated into the α-SiAlON, will form the stable liquid. The ratio (*K*) of the amount of Y_2O_3 to the amount of Y_2O_3 incorporated into the α-SiAlON was calculated to be 1.2, 1.43, 1.61, 1.69, 1.94 and 2.36 (Table 1). This ratio was used as a parameter for the amount of additional liquid phase because this ratio is 1 for the composition in the α-/β-SiAlON plane. Of course the Y_2O_3 will not form the liquid phase on its own during sintering, SiO_2, Al_2O_3, Si_3N_4 and AlN will also be dissolved.

The starting powders were weighed and milled in water-free isopropanol for 6 h in an agate jar using agate milling media. The mixed powders were dried and isostatically pressed into bars with dimensions 60×20×20 mm under a pressure of 200 MPa. In Fig. 1 the compositions are shown with respect to the homogeneity range of the α-SiAlONs, determined by Herrmann et al.[10] that the solubility area of the Y-α-SiAlON was extended to lower *x* values than those suggested in the literature.

Sintering was carried out in a gas pressure sintering furnace (in DS1/150/2000, KCE) in a nitrogen atmosphere (50 bar). Three different sintering procedures were used. One series of samples was heated directly to 1825°C and then held for 3 h. The temperature was raised at 20°C/min to 1100°C and 10°C/min thereafter. The second and third group of samples were held at 1500 or 1600°C for 1 h before the final sintering step at 1825°C for 3 h. The heating rate used in this sintering cycle was the same as

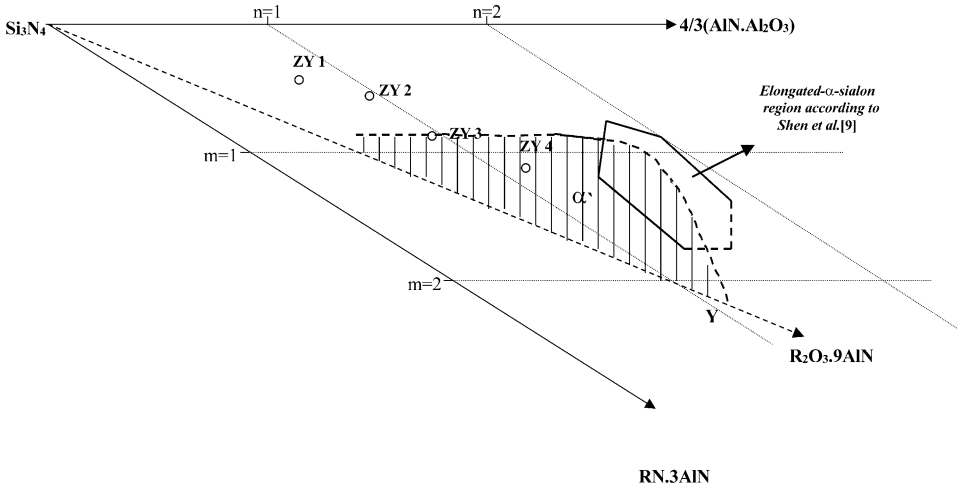

Fig. 1. Composition of samples with respect to the α-SiAlON homogeneity range.[10]

in the sintering cycle without an intermediate holding step. The cooling rate of the furnace was estimated to be about 20°C/min.

The density of the samples was measured by the Archimedes method. The results obtained after sintering are given in Table 2. The surface of the sintered samples was removed (at least 4 mm) and then the phase composition was analysed by the X-ray diffraction technique (XRD 7 Seifert, FPM; Cu K_α). Quantitative XRD analysis and the determination of the occupation factors were made with the programme REFINE++(Seifert FPM).[11] The results are given in the Table 2. Microstructural characterisation was performed with a scanning electron microscope (Cambridge Instruments Stereo Scan 260). The samples for SEM examination were prepared by two methods. For samples with low a density, the fracture surfaces were investigated. Dense samples were polished and etched in molten NaOH for 15–100 s. All samples were coated with gold prior to SEM observation. For mechanical test analyses, hardness and fracture toughness were measured using a Vickers diamond indenter on the polished surface with a 10 kg load. K_{IC} values were calculated using the following formula:[12,13]

$$K_{IC}[\mathrm{MPam}]^{1/2} = k(E/H)^{1/2} \ {}^{*}F^{*}c^{-3/2} \ {}^{*}0.0316$$

Table 2
Density and phase assemblage of samples fired at different temperatures for 3 h[a]

Sample	m	n	K	Sintering conditions	x (from m)	Density (g/cm^3)	m	Phase composition	x-Measured	z-Value β-SiAlON
ZY 1	0.44	0.76	1	1825°C/3h	0.147	1.766	0.41	58.7α′-41.3β′	0.24	0.35
				1500°C/1 + 1825°C/3h	0.147	1.761	0.30	61.2α′-38.77β′	0.30	0.35
				1600°C/1 + 1825°C/3h	0.147	1.701	3.84	59.2α′-40.8β′	0.23	0.35
ZY 1b	0.44	0.76	1.43	1825°C/3h	0.147	2.204	0.63	70.7α′-29.3β′	0.25	0.37
				1500°C/1 + 1825°C/3h	0.147	2.224	0.45	72.8α′-27.2β′- Y_2SiO_5(vw)	0.26	0.37
				1600°C/1 + 1825°C/3h	0.147	2.050	0.72	72.6α′-27.4β′- Y_2SiO_5(w)	0.27	0.39
ZY 1f	0.44	0.76	2.36	1825°C/3h	0.147	3.274	0.47	81.4α′-17.2β′- 1.4 Y-N-Apatite	0.26	0.26
				1500°C/1 + 1825°C/3h	0.147	3.272	0.40	81.9α′-16.6β′- 1.5Y-N-Apatit	0.24	0.31
ZY 2	0.59	0.98	1	1825°C/3h	0.197	1.980	0.79	69.9α′-30.06β′	0.45	0.46
				1500°C/1 + 1825°C/3h	0.197	1.976	0.63	72.6α′-27.4β′	0.32	0.43
				1600°C/1 + 1825°C/3h	0.197	1.980	0.73	62.4α′-37.6β′	0.5	0.43
ZY 2b	0.59	0.59	1.43	1825°C/3h	0.197	3.090	0.56	92.1α′-7.9β′- Y_2SiO_5(w)	0.27	0.47
				1500°C/1 + 1825°C/3h	0.197	2.933	0.53	91.7α′-8.3β′- Y_2SiO_5(w)	0.27	0.47
				1600°C/1 + 1825°C/3h	0.197	2.849	0.04	91.2α′-8.8β′- Y_2SiO_5(vw)	0.34	0.45
ZY 2c	0.59	0.98	1.61	1825°C/3h	0.197	3.263	0.66	93.7α′-6.4β′	0.26	0.39
				1500°C/1 + 1825°C/3h	0.197	3.245	0.61	93.2α′-6.8β′	0.26	0.42
ZY 2e	0.59	0.98	1.94	1825°C/3h	0.197	3.276	0.67	96.3α′-3.7β′	0.26	0.37
				1500°C/1 + 1825°C/3h	0.197	3.278	0.48	95.7α′-4.3β′	0.26	0.37
ZY 3	0.91	0.98	1	1825°C/3h	0.303	1.936	0.91	98.7α′-1.3β′	0.31	0.23
				1500°C/1 + 1825°C/3h	0.303	1.872	0.80	98.7α′-1.3β′	0.30	0.36
				1600°C/1 + 1825°C/3h	0.303	1.932	0.77	97.8α′-2.2β′	0.43	0.32
ZY 3b	0.91	0.98	1.43	1825°C/3h	0.303	3.287	0.55	100α′-Y_2SiO_5(w)	0.35	
				1500°C/1 + 1825°C/3h	0.303	3.307	0.45	97.5α′-2.2YAM-0.29Y-N-Apatit	0.36	
				1600°C/1 + 1825°C/3h	0.303	3.083	0.48	98.6α′-1.4 Y-N-Apatite	0.35	
ZY 3d	0.91	0.98	1.69	1825°C/3h	0.303	3.314	0.62	97.7α′-2.3 Y-N-Apatite	0.37	
				1500°C/1 + 1825°C/3h	0.303	3.313	0.63	98.8α′-1.2Y-N-Apatit	0.37	
ZY 4	1.12	1.17	1	1825°C/3h	0.373	2.240	0.65	100α′	0.36	
				1500°C/1 + 1825°C/3h	0.373	2.246	0.46	100α′	0.36	
				1600°C/1 + 1825°C/3h	0.373	2.251	0.50	100α′	0.37	
ZY 4a	1.12	1.17	1.2	1825°C/3h	0.373	3.271	0.46	100α′	0.42	
				1500°C/1 + 1825°C/3h	0.373	2.916	0.70	100α′-Y_2SiO_5(vw)	0.44	
				1600°C/1 + 1825°C/3h	0.373	2.908	0.65	100α′- Y_2SiO_5(vw)	0.42	
ZY 4b	1.12	1.17	1.43	1825°C/3h	0.373	3.314	0.46	100α′	0.43	
				1500°C/1 + 1825°C/3h	0.373	3.305	0.65	98.1α′-1.9 Y-N-Apatite	0.43	
				1600°C/1 + 1825°C/3h	0.373	3.298	0.56	98.3α′-1.7 Y-N-Apatite	0.43	
ZY 5	0.86	1.26	1	1825°C/3h	0.286	2.141	0.86	98.8α′-1.2β′	0.30	0.59
ZY 6	1	1.26	1	1825°C/3h	0.333	2.281	0.61	100α′	0.36	
ZY 7	1.16	1.26	1	1825°C/3h	0.386	2.379	0.71	100α′	0.40	
ZY 8	1.0	1.5	1	1825°C/3h	0.333	2.376	0.72	100α′	0.36	
ZY 9	1.4	1.5	1	1825°C/3h	0.467	3.223	0.57	100α′	0.48	
ZY 10	1.8	1.5	1	1825°C/3h	0.6	3.284	0.39	100α′	0.57	

[a] α′: $Y_x^{+v}Si_{12-(m+n)}Al_{m+n}O_nN_{16-n}$; β′: $Si_{6-z}Al_zO_zN_{8-z}$; YAM: $A_2Y_4O_9$; YAG: $A_5Y_3O_{12}$; M: $Y_2Si_3N_4O_3$; NYAM: $Y_{10}A_2Si_3O_{18}N_4$; w: weak; vw: very weak; *m*: weight loss.

E = Young's modulus (320 GPa), H = hardness (GPa), F = load (N), c = crack length (μm), k = dimensionless constant 0.016±0.004.

$$H_V(\text{GPa}) = \frac{0.47^* P}{a^2}$$

P = applied force(10 kg), a = half of the length of the diagonal indentation.

3. Results and discussion

3.1. Densification behaviour

The dilatometric study was performed using samples ZY 3, 3b and 3d with a linear heating rate of 10°C/min under nitrogen gas at an ambient pressure (Fig. 2a). The derived shrinkage rate (Fig. 2b) was explained by taking the phase composition into account. In samples ZY 3b and 3d, shrinkage starts at 1200°C. As the temperature was increased, the sintering rate curve showed three maxima. The first at 1250°C corresponds to rearrangement of the particles. The second one occurs at around 1550°C. At this temperature, the highest shrinkage rate was observed. At 1400–1500°C, Y_2O_3 and Al_2O_3 were dissolved in the liquid phase, although they could not be detected by XRD. Very little AlN was dissolved at this temperature (Table 3). Apatite was observed as a crystalline phase, which was properly formed during cooling. The consequence of this finding is that a high amount of low-viscosity liquid was formed at 1500–1550°C, allowing fast densification to occur. With a further increase in temperature, enhanced α-SiAlON formation was observed (see 1600°C, Table 3). This process is connected with a reduction in the amount of liquid phase. At higher temperatures, the viscosity of the remaining liquid was reduced and the amounts of α-Si_3N_4 and α-SiAlON, which were dissolved in the liquid, were increased. This led to additional shrinkage in samples ZY 3b and ZY 3d with a higher amount of liquid phase at 1700–1800°C. In sample ZY 3, which had no additional liquid, the densification rate at >1650°C was very low because no more liquid existed after complete α-SiAlON formation occurred. This is also an explanation for the low density of the samples with additional liquid that were sintered at 1825°C (Table 2).

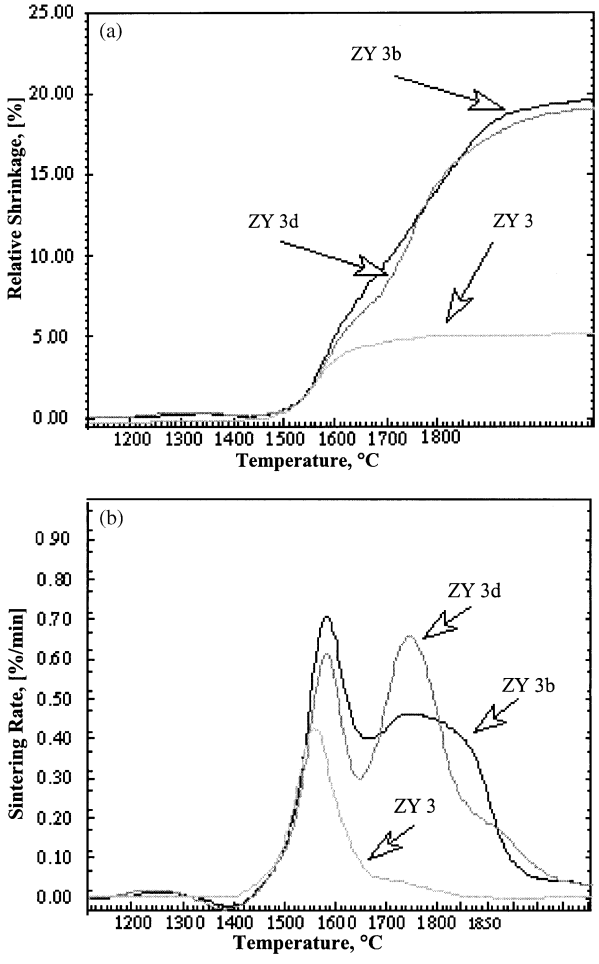

Fig. 2. (a) Change in the density of the investigated compositions as a function of temperature. (b). Derived sintering rate of the investigated compositions as a function of temperature.

The densification behaviour in the temperature range up to 1600°C was very similar to that observed by Greil et al.,[14] who found garnet as an intermediate phase. The lower sintering rate at higher temperature was correlated with the formation of the melilite type phase. This was not the case in our investigations. The differences are associated with the lower n and m values in our compositions.

Fig. 3 shows the relationship between density and amount of additional Y_2O_3 for samples which were sintered at 1825°C/3 h. It can be seen from the figure that the density increases with an increasing amount of liquid phase (i.e. increasing K). ZY 4 possessed the highest and ZY 1 possessed the lowest densities. The difference in densities can be explained by the starting composition. If the composition is close to the Si_3N_4

Table 3
Phase analysis results of ZY 3, 3b and 3d at a low sintering temperatures

Sample	Sintering condition	Phase composition
ZY 3	1400°C/5 min	83.32α-10.96AlN-5.72 $Y_{10}A_2Si_3O_{18}N_4$
	1500°C/5 min	84.61α-10.99AlN-4.40$Y_{10}A_2Si_3O_{18}N_4$
	1600°C/5 min	46.89α′-48.67α-4.45AlN
ZY 3b	1400°C/5 min	81.08α-11AlN-7.93 $Y_{10}A_2Si_3O_{18}N_4$
	1500°C/5 min	83.62α-9.25AlN-7.12 $Y_{10}A_2Si_3O_{18}N_4$
	1600°C/5 min	28.81α′-59.64α-7.14AlN
ZY 3d	1400°C/5 min	79.84α-10.04AlN-10.12 $Y_{10}A_2Si_3O_{18}N_4$
	1500°C/5 min	81.98α-9.5AlN-8.52 $Y_{10}A_2Si_3O_{18}N_4$
	1600°C/5 min	35.53α′-53.69α-5.79AlN-4.99 $Y_{10}A_2Si_3O_{18}N_4$

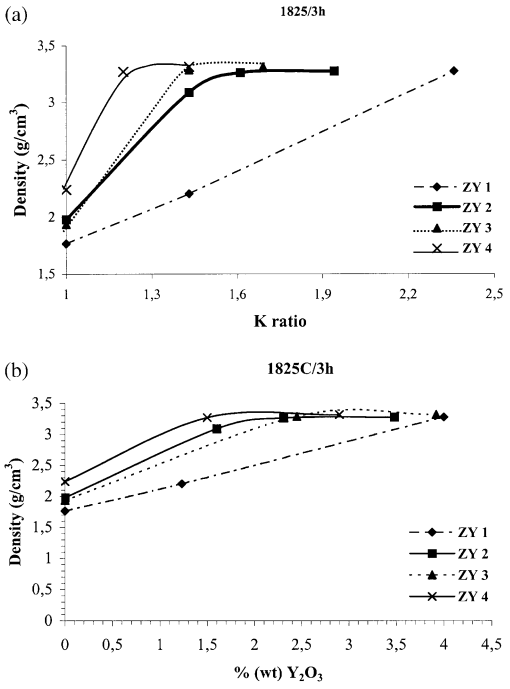

Fig. 3. (a) Relationship between density and K ratio. (b) Relationship between density and additional amount of Y_2O_3.

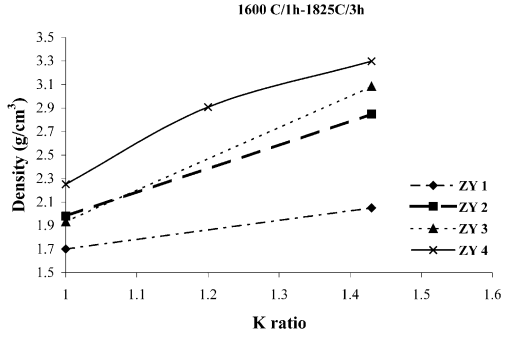

Fig. 4. Dependency of density on the amount of additional liquid phase (changed heating cycle-additional holding time at 1600°C/1 h).

corner (low m and n values), the amount of transient liquid during densification is low and a higher amount of additional liquid phase is necessary to reach the same density. Even when the same amount of additional Y_2O_3 is added to different samples the density is lower for the samples with a lower amount of transient liquid (Fig. 3b). Fig. 4 illustrates the effect of an additional holding time at 1600°C for 1 h. In this case, the final density is lower than those of samples sintered at 1825°C. During the holding stage at 1600°C, α-SiAlON was formed and the amount of liquid phase was significantly reduced (Table 4). According to Table 2, an α-SiAlON richer in Y was formed at 1600°C than at higher temperatures (except ZY 1). This effect is so pronounced that the higher x values were also observed in the sintered α-SiAlONs with a holding step at 1600°C (ZY 2, 2b and ZY 3). In these cases, the amount of liquid phase is too low for complete recrystallization at high temperatures to occur and the composition of the α-SiAlON is not at equilibrium. A dependence of the x values on the sintering conditions is found for all samples without an additional liquid phase and with a low amount of transient liquid. In these cases, the different x values were probably caused by kinetics. This behaviour also makes the determination of the phase relationships difficult in this part of the system. With increasing the amount of the stable liquid phase the variation in the x values for the different sintering conditions is significantly reduced, because enough liquid exists for the recrystallization of the material.

The behaviour was similar for the samples with an additional isothermal heating step at 1500°C. But at this temperature, α-SiAlON formation was not as pronounced (only one-third of the α-Si_3N_4 was converted). This is why the influence on the final densities was much lower for these samples than for samples with a higher holding temperature (Fig. 5).

Two different groups of samples were prepared to show the effect of liquid phase on densification when $K=1$ (ratio of Y_2O_3 to amount of Y_2O_3 incorporated into α-SiAlON) (Fig. 8). One group was selected from the α-β-SiAlON and α-SiAlON solid solubility area (ZY 5, ZY 6 and ZY 7). Another group was at the oxygen-rich boundary of the solid solubility area of the α-SiAlON. The results show that the density increases up to theoretical values with increasing m values for the materials with high n values, i.e. a high amount of transient

Table 4
Results of the phase analysis in the system after heating at 1600°C for 1 h

Sample	m	n	K	x (from m)	x-Measured	Phase composition
ZY 1	0.44	0.76	1	0.147	0.235	59.2α′-40.8β′
ZY 1b	0.44	0.76	1.43	0.147	0.323	72.6α′-27.4β′- Y_2SiO_5 (w)
ZY 2	0.59	0.98	1	0.197	0.5	62.4α′-37.6β′
ZY 2b	0.59	0.59	1.43	0.197	0.336	91.2α′-8.8β′- Y_2SiO_5 (vw)
ZY 3	0.91	0.98	1	0.303	0.435	97.8α′-2.2β′
ZY 3b	0.91	0.98	1.43	0.303	0.348	98.6α′-1.4 Y-N-apatite
ZY 4	1.12	1.17	1	0.373	0.366	100α′
ZY 4a	1.12	1.17	1.2	0.373	0.416	100α′- Y_2SiO_5 (vw)
ZY 4b	1.12	1.17	1.43	0.373	0.429	98.3α′-1.7 Y-N-apatite

liquid, whereas the samples with low n and m values can not be densified without an additional amount of the liquid phase (Fig. 6).

By increasing the amount of additional Y_2O_3 in the series of samples ZY 1-1f and ZY 2-e, the α-SiAlON/(α-SiAlON + β-SiAlON) ratio could also be increased (Table 2, Fig. 7). The observed x values did not change significantly with increasing amount of additional Y_2O_3. An exception was made by sample ZY 2, which was not at in equilibrium. This behaviour can be explained using the phase diagram. In Fig. 8, it is shown schematically how the composition changes with Y_2O_3 additions. Assuming that the composition of the liquid phase shifts only slightly when additional amounts of Y_2O_3 are used and the composition of the liquid phase is rich in Al_2O_3 and SiO_2, it is obvious, that the α-SiAlON content in the samples in the α/β-SiAlON region has to increase with an increasing amount of Y_2O_3. The same shift in the α-SiAlON composition must occur in the samples which contain α-SiAlON and a glassy phase (ZY 4-4b). The data show that in this case, the x values are not constant, but shift from 0.36 for $K=1$ to 0.43 for $K=1.43$. The same behaviour is exhibited by samples ZY 3, 3b and 3d. XRD analysis (Table 2, samples ZY 1, 1b, 1f, ZY 2e) shows that the samples in the three phase region of α-SiAlON/β-SiAlON-liquid have an x value,

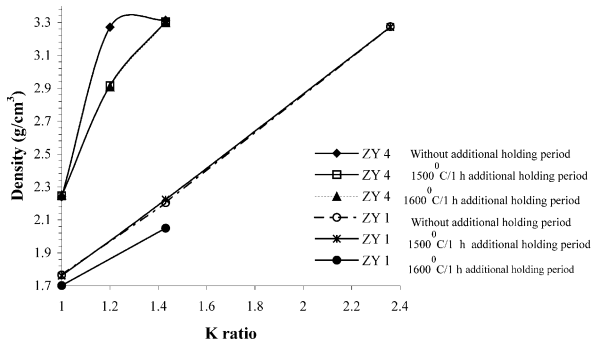

Fig. 5. The effect of the sintering condition and additive ratio on the density. (The heating stage was varied: — continuous heating at 10 K/min; — additional holding period at 1600°C/1 h or 1500°C/1 h).

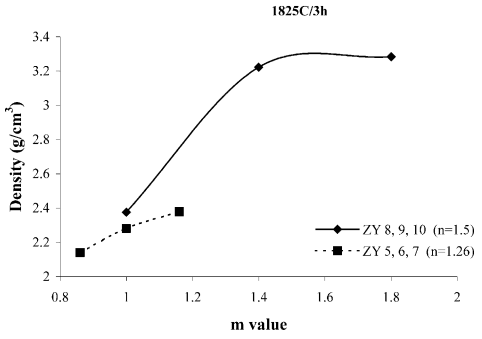

Fig. 6. Relationship between m value and density for a constant additives ratio ($K=1$) (heating at 10 K/min).

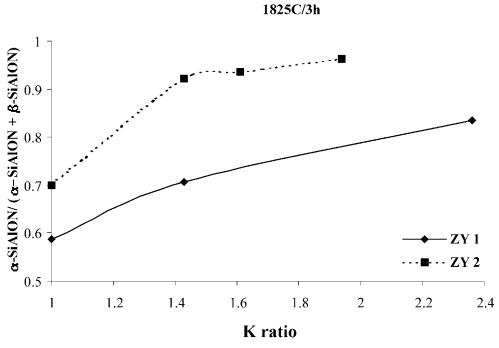

Fig. 7. Change in the amount of α-SiAlON as a function the amount of additives (heating: 10 K/min up to 1825°C; holding time: 3 h).

Table 5
Hardness, toughness and strength of the materials

Sample	K	$\alpha/(\alpha+\beta)$ (%)	Sintering condition	HV10	K_{IC}[b] (MPam$^{1/2}$)	Strength (MPa)
ZY 1f	2.36	81	1825°C/3h	1878±26	4.4	–
	–		1500°C/1h→1825°C/3h	1824±34	4.2	638±15
ZY 2c	1.61	93.7	1825°C/3h	1976±38	5.3	–
	–		1500°C/1h→1825°C/3h	1880±23	5.6	599±75
ZY 2e	1.94	96.3	1825°C/3h	1923±50	5.4	–
	–		1500°C/1h→1825°C/3h	1962±37	5.0	676±35
ZY 3b	1.43	100	1825°C/3h	1808±33	5.4	–
	–		1500°C/1h→1825°C/3h	1856±50	4.4	532±50
ZY 3d	1.69	100	1825°C/3h	1869±26	3.9	–
	–		1500°C/1h→1825°C/3h	1864±30	3.5	491±70
ZY 4a	1.2	100	1825°C/3h	1823±34	6.0	–
ZY 4b	1.43	100	1825°C/3h	1871±25	4.3	–
	–		1600°C/1h→1825°C/3h	1865±28	4.8	–
	–		1500°C/1h→1825°C/3h	1817±38	3.9	–
Comparison[a]		0		1480±40	5.2	920±40

[a] β-Si_3N_4 material with 6 wt.% Y_2O_3/4 wt.% Al_2O_3.
[b] Standard deviation of the values 0.1 MPam$^{1/2}$.

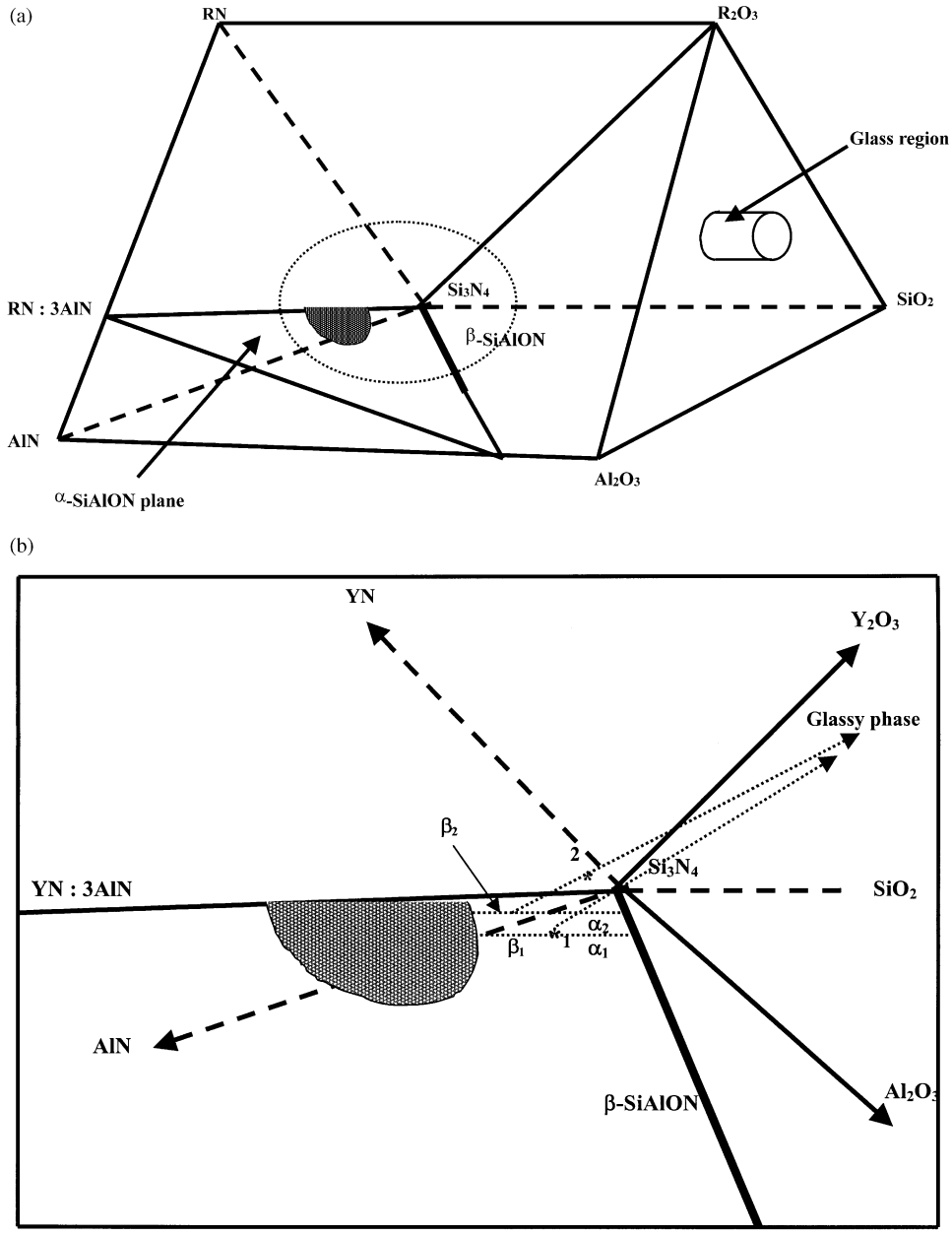

Fig. 8. (a) Jänecke prism of oxynitride system of silicon, aluminum and *R* (where *R* is a rare-earth cation). (b) shematic illustration of the change in the phase composition as a result of the addition of Y_2O_3 to the sample [1 Composition without additional liquid, α-SiAlON content is $\alpha_1/(\alpha_1+\beta_1)$; 2 composition with additional Y_2O_3, the corresponding ratio of α-SiAlON is $\alpha_2/(\alpha_2+\beta_2)$].

which is much lower than the lowest value reported in the literature. The *x* value does not depend on the amount of additional liquid (*K* value). This data can only be explained assuming that the homogeneity range of the α-SiAlONs toward Si_3N_4 is at higher temperatures and lower *n* values than were found in literature.

4. Morphology of the α-SiAlON ceramics

The α-SiAlON formation process can be divided into two steps, nucleation and growth. When α-Si_3N_4 is used as the starting powder, formation of α-SiAlON nuclei most likely occurs by epitaxial growth of the α-SiAlON on the α-Si_3N_4. The growth of the α-SiAlON grains mostly depend on the amount and composition of the liquid phase during sintering.

Figs. 9 and 10 show the influence of the amount of additional liquid on the grain size and grain shape. The microstructures of samples ZY 1 and ZY 3 are similar to those of samples ZY 4 and ZY 2. Without additional liquid phase, the materials are porous and have equiaxed grains (see Figs. 9a and 10). With increasing amount of additional Y_2O_3, anisotropic grain growth takes place, the grains become elongated and full density were achieved (Fig. 9b and c).

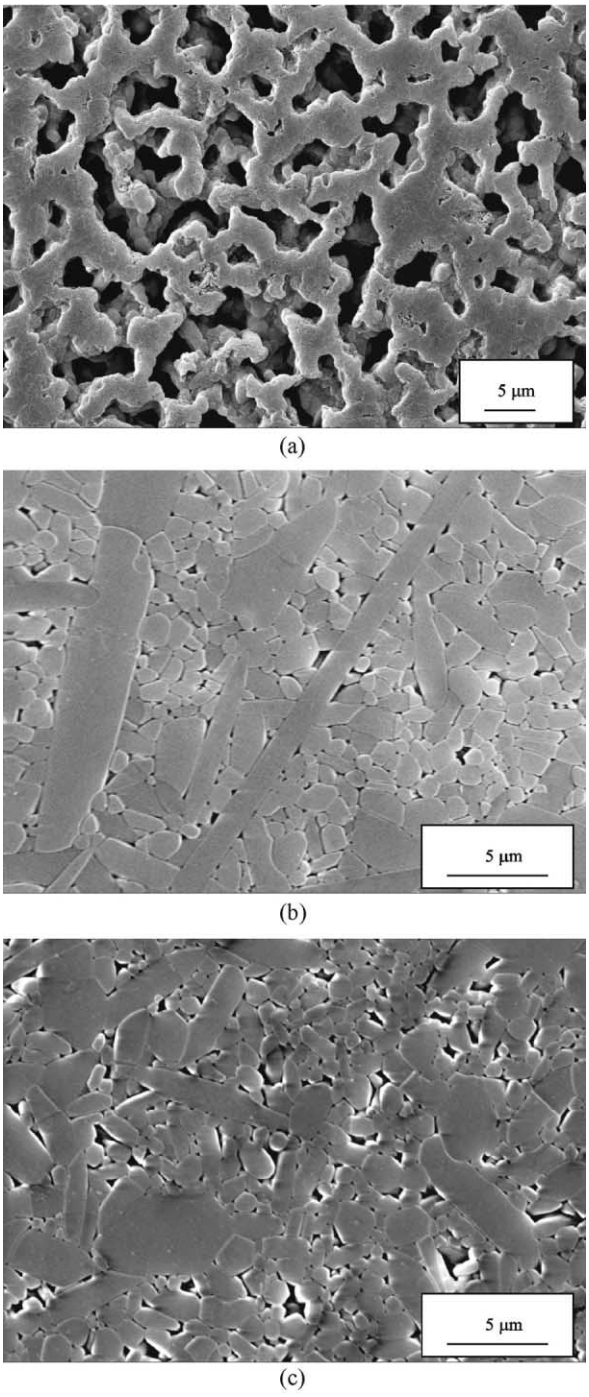

Fig. 9. Secondary electron micrograph of the polished surface from ZY 2 sintered at 1825°C/3 h, (a) $K=1$, (b) $K=1.61$, (c) $K=1.94$.

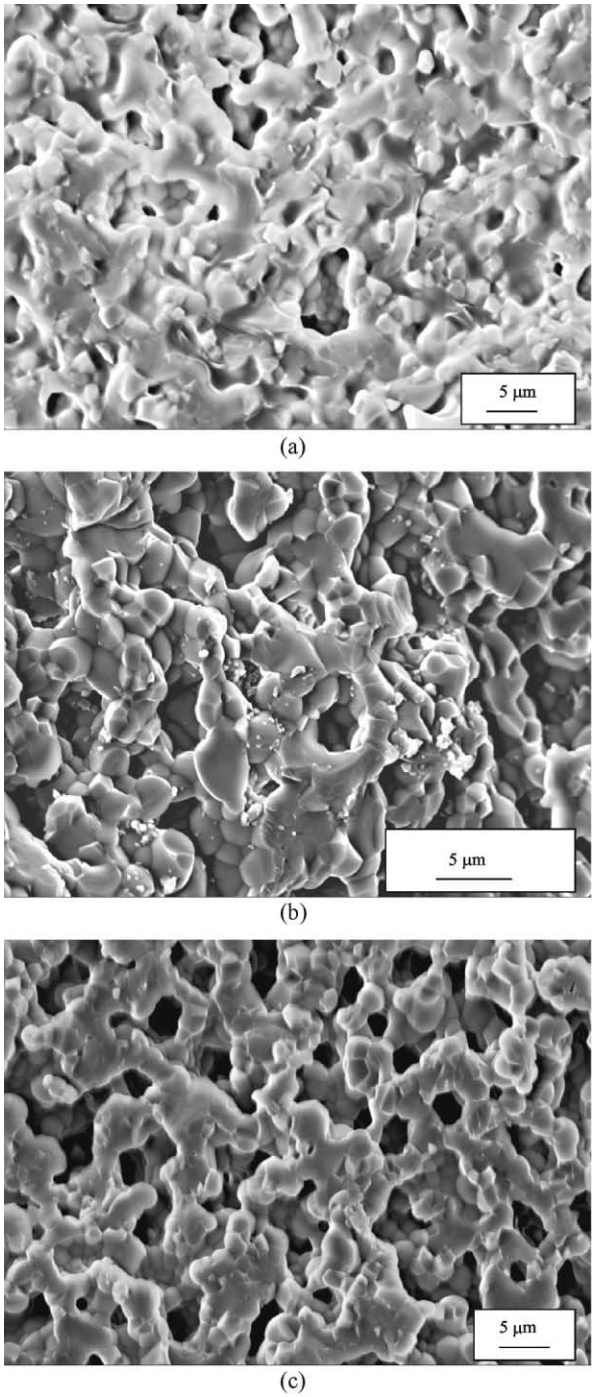

Fig. 10. Secondary electron micrograph of the fracture surface from ZY 4, (a) with heating rate 10 K, sintered 1825°C/3 h; (b) with additional holding period at 1500°C/1 h; (c) with additional holding period at 1600°C/1 h.

The investigated compositions have relative low n and m values. That is why the amount of the transient liquid is insufficient for anisotropic grain growth and densification to occur. The additional holding period at 1500 or 1600°C before the sintering temperature is reached does not change this behaviour significantly. By increasing the amount of the liquid phase, the length, the thickness and the amount of elongated grains increase. With an increasing amount of the liquid phase (samples ZY 2-2e with $K=1.94$) the grain size increases. Besides the amount of liquid phase, the sintering conditions also affect the formation of elongated α-SiAlON grains. Large elongated grains were observed for the samples which contained an additional liquid phase and which did not undergo a holding period at low temperatures (Figs. 11a and b and 12a). In the samples which were

held 1 h at 1600°C, the amount of large grains was reduced (Fig. 12b and c). This is because most of the α-SiAlON is formed at the lower temperature (see Table 4), where grain growth is not as pronounced and is more homogeneous. During the subsequent sintering steps, a lower amount of transient liquid for the growth of α-SiAlON exists. These qualitative findings have to be proven by quantitative measurements. All of the results show that the liquid phase is a very important factor for the formation of the microstructure. In samples with no additional liquid, grain growth can occur only when a transient liquid is present. The amount of transient liquid is higher when higher *n* and *m* values are used. For these compositions, elongated grain growth occurs without the need for a higher amount of liquid phase. The amount of transient liquid at high temperatures depends on the reaction path at lower sintering temperatures, besides on the composition. Elongated grain growth can be enhanced if the formation of α-SiAlON at low temperatures is reduced, e.g. by using a fast heating rate or by reducing the amount of growing grains by using ß powders or mixed cations.

5. Mechanical properties α-SiAlON

All samples with a high amount of α-SiAlON have the typical high hardness values that all α-SiAlONs have. Mechanical properties of studied samples are given in Table 5. In samples ZY 2-2e the hardness decreases with increasing amounts of α-SiAlON and additional additive. In the series ZY 3 and ZY 4, the hardness increases with increasing amount of additives (constant amount of α-SiAlON). The K_{IC} values are generally lower for samples with a high amount of stable liquid (high *K*) than for samples with a lower amount (except for ZY 2 series, which have a low amount of transient liquid). Comparing α-SiAlON materials with a standard β-Si_3N_4 material (6% Y_2O_3/4% Al_2O_3), it is obvious, that samples with an optimal composition show the same results as the β materials. The influence of the composition on the fracture toughness is not well understood and needs to be investigated further. The strengths of the α-SiAlON materials are lower than those of the β-Si_3N_4 materials. Strength-determining defects are pores, which can be connected with a locally reduced amount of liquid phase.

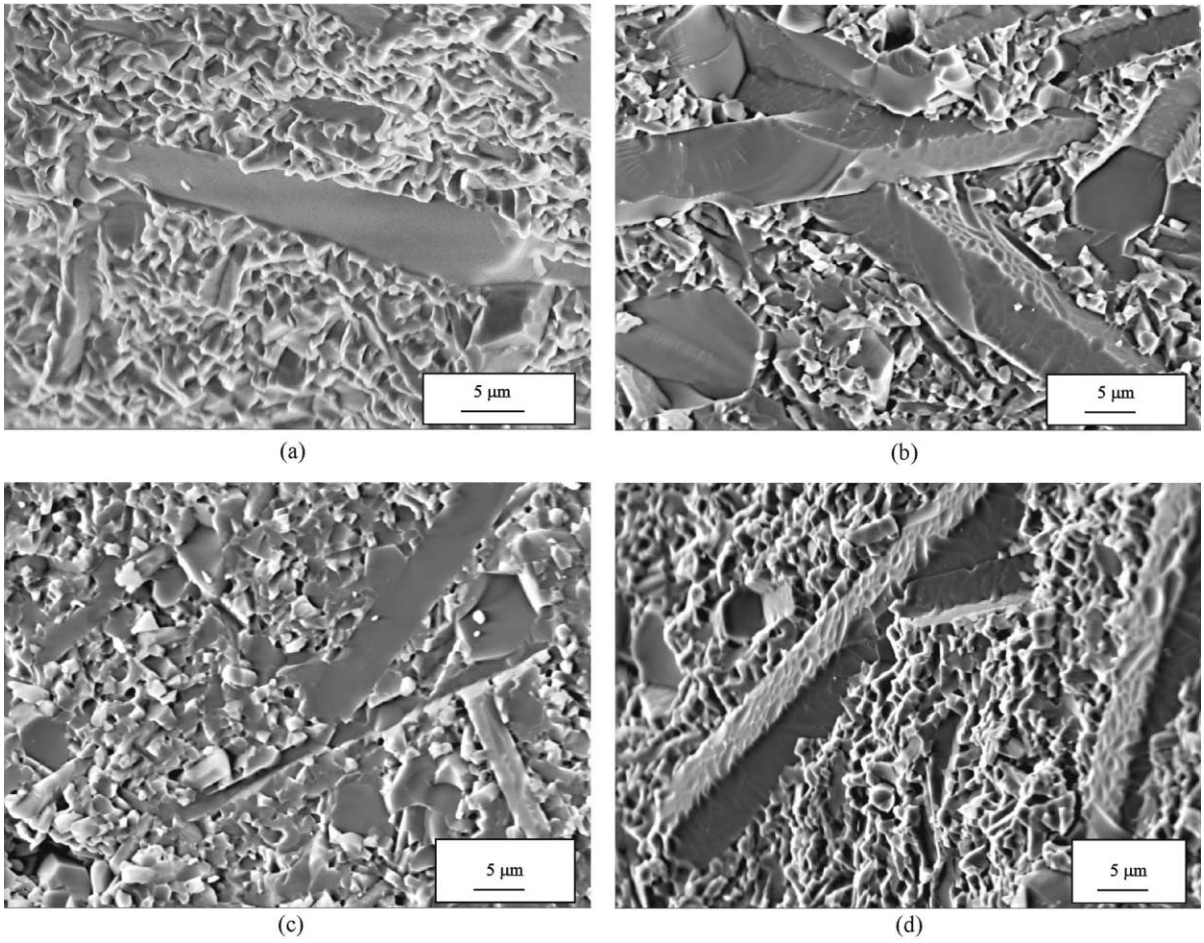

Fig. 11. Secondary electron micrograph of the fracture surface from ZY 4 sintered at 1825°C/3 h; (a) $K = 1.2$, (b) $K = 1.43$, (c) with additional holding period at 1500°C/1 h, $K = 1.43$, (d) with additional holding period at 1600°C/1 h, $K = 1.43$.

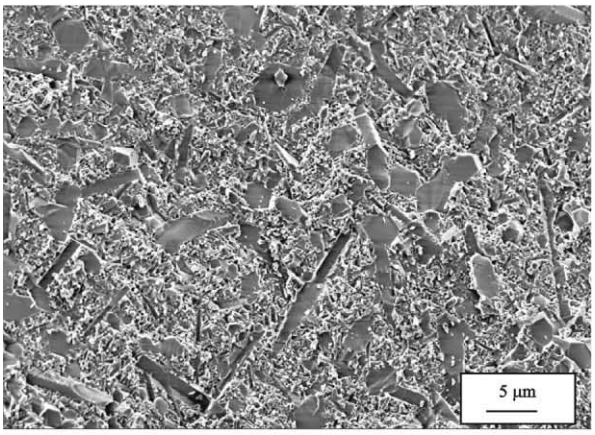

(a)

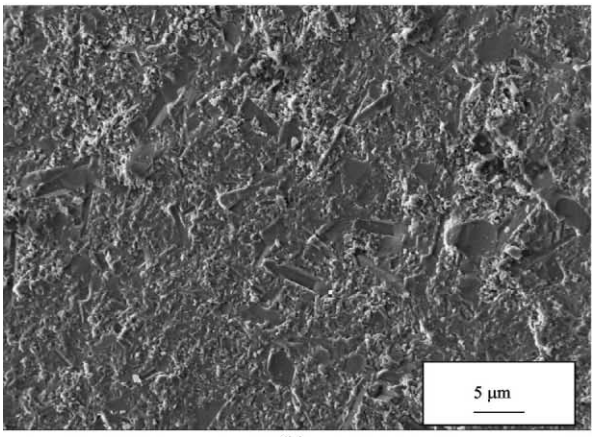

(b)

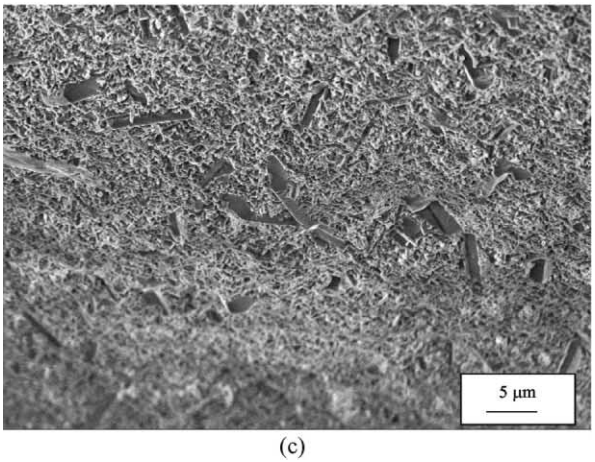

(c)

Fig. 12. Secondary electron micrograph of the fracture surface from ZY 4 sintered at 1825°C/3 h ($K=1.43$); (a) heating up 10 K/min, (b) with additional holding period at 1500°C/1 h, $K=1.43$, (c) with additional holding period at 1600°C/1 h, $K=1.43$.

6. Conclusions

- The densification behaviour and the microstructure of yttrium α-SiAlON ceramics with different amount of additional stable liquid were investigated. The amounts of stable liquid were controlled by the Y_2O_3 added to the SiAlON composition.
- A strong correlation was found between the amount of additional liquid, the densification behaviour and the microstructural formation. Samples with low n and m values can only be densified to full density when an additional amount of the stable liquid phase exists.
- The presence of an additional amount of liquid phase causes elongated grain growth of the α-SiAlON materials with low n and m values ($m<1$; $n<1$) at a sintering temperature of 1825°C.
- Yttrium α-SiAlON ceramics were fabricated by GPS with or without an additional holding step at 1500 or 1600°C during heating to the sintering temperature of 1825°C. When an additional holding step during heating was used, the final density was lower than that of samples with continuous heating. The reason for this behaviour is that during the holding time at low temperatures, formation of α-SiAlON starts. The formed α-SiAlON reduces the amount of liquid phase available for densification at high temperatures. The effect of the sintering procedure on the densification behaviour decreases with increasing amount of additional stable liquid phase.
- The intermediate holding step during heating leads to a more uniform microstructure. The amount of large elongated grains is reduced.
- The materials exhibited high hardness values of greater than 1800 (HV10), which are typical for α-SiAlON.
- The dense samples with elongated grains exhibited a high fracture toughness which is comparable with the toughness of the ß-Si_3N_4 materials.
- The strength of the materials is somewhat lower for the α-SiAlON materials than for the ß-Si_3N_4 materials. This is connected with a higher defect size resulting from inhomogeneous α-SiAlON formation.

Acknowledgements

One of the authors (S.K.) would like to acknowledge financial assistance from the Deutscher Akademischer Austausch-Dienst (DAAD, Germany), financing partially the research which was carried out at the IKTS.

References

1. Mitomo, M. and Petzow, G., (Guest Editors), Recent progress in silicon nitride and silicon carbide ceramics. *MRS Bull.*, 1995, **2**, 19-41.

2. Becher, P. F., Hwang, S. L., Lin, H. T. and Tiegs, T. N., Microstructure contributions to the fracture resistance of silicon nitride ceramics. In *Tailoring of Mechanical Properties of Si3N4 Ceramics*, ed. M. J. Hoffmann and G. Petzow. Kluwer Academic, Dordrecht, The Netherlands, 1994, pp. 87–100.
3. Cao, G. Z. and Metselaar, R., α-SiAlON ceramics: a review. *Chem. Mater.*, 1991, **3**(2), 242–252.
4. Hwang, C. J., Susintzky, D. W. and Beaman, D. R., Preparation of multication α-sialon containing strontium. *J. Am. Ceram. Soc.*, 1995, **78**, 588.
5. Wang, H., Cheng, Y.-B., Muddle, B. C., Gao, L. and Yen, T. S., Preferred orientation in hot-pressed Ca α-SiAlON ceramics. *J. Mater. Sci. Lett.*, 1996, **15**, 447–449.
6. Nordberg, L. O., Shen, Z., Nygren, M. and Ekstrom, T., On the extension of the α-SiAlON solid solution range and anisotropic grain growth in Sm-Doped α-SiAlON ceramics. *J. Eur. Ceram. Soc.*, 1997, **17**, 575.
7. Chen, I.-W. and Rosenflanz, A., A tough SiAlON ceramics based on α-Si_3N_4 with a wisker-like microstructure. *Nature*, 1997, **389**(16), 701–704.
8. Mandal, H., New developments in α-SiAlON ceramics. *J. Eur. Ceram. Soc.*, 1999, **19**, 2349–2357.
9. Shen, Z. J., Nordberg, L-O., Nygren, M. and Ekström, T., α-SiAlON grains with high aspect ratio — Utopia or Reality. In *Engineering Ceramics'96; Higher Reliability Trough Processing*, ed. G. N. Babini, M. Haviar and P. Sajgalik. Kluwer Academic, The Netherland, 1997, pp. 169–177.
10. Herrmann, M., Kurama, S. and Mandal, H., Investigation of the phase composition and stability of the α-SiAlON by Rietveld method. *J. Eur. Ceram. Soc.*, submitted.
11. Taut, T. and Bergmann, J. Rietveld-Analyse mit dem Programmsystem Refine + +. *Handbuch der Version 1.1*.
12. Amin, K. E., Thoughness, hardness and wear. *Engineering Materials Handbook Ceramics and Glasses*, Vol. 4. ASM International, 1991, p. 601.
13. Evans, A. G. and Charles, E. A., Fracture toughness determinations by indentation. *J. Am. Ceram. Soc.*, 1976, **59**, 371.
14. Greil, P., Nagel, A., Stutz, D. and Petzow, G., Reaction sintering of α-Si_3N_4 based ceramics. In 7. *German–Yugoslavian Symposium on Advanced Materials*, 1985.